Research Article

Rapid Communications in Mass Spectrometry

Received: 6 March 2014 Revised: 1 May 2014 Accepted: 21 May 2014 Published online in Wiley Online Library

Rapid Commun. Mass Spectrom. **2014**, 1716–1722
(wileyonlinelibrary.com) DOI: 10.1002/rcm.6952

Contribution of thermal energy to initial ion production in matrix-assisted laser desorption/ionization observed with 2,4,6-trihydroxyacetophenone

Yin-Hung Lai[1], Bo-Gaun Chen[2], Yuan Tseh Lee[1], Yi-Sheng Wang[1]* and Sheng Hsien Lin[2,3]**

[1]Genomics Research Center, Academia Sinica, Taipei 115, Taiwan
[2]Institute of Atomic and Molecular Sciences, Academia Sinica, Taipei 10617, Taiwan
[3]Department of Applied Chemistry, National Chiao Tung University, Hsinchu 30010, Taiwan

RATIONALE: Although several reaction models have been proposed in the literature to explain matrix-assisted laser desorption/ionization (MALDI), further study is still necessary to explore the important ionization pathways that occur under the high-temperature environment of MALDI. 2,4,6-Trihydroxyacetophenone (THAP) is an ideal compound for evaluating the contribution of thermal energy to an initial reaction with minimum side reactions.
METHODS: Desorbed neutral THAP and ions were measured using a crossed-molecular beam machine and commercial MALDI-TOF instrument, respectively. A quantitative model incorporating an Arrhenius-type desorption rate derived from transition state theory was proposed. Reaction enthalpy was calculated using *GAUSSIAN 03* software with dielectric effect. Additional evidence of thermal-induced proton disproportionation was given by the indirect ionization of THAP embedded in excess fullerene molecules excited by a 450 nm laser.
RESULTS: The quantitative model predicted that proton disproportionation of THAP would be achieved by thermal energy converted from a commonly used single UV laser photon. The dielectric effect reduced the reaction Gibbs free energy considerably even when the dielectric constant was reduced under high-temperature MALDI conditions. With minimum fitting parameters, observations of pure THAP and THAP mixed with fullerene both agreed with predictions.
CONCLUSIONS: Proton disproportionation of solid THAP was energetically favorable with a single UV laser photon. The quantitative model revealed an important initial ionization pathway induced by the abrupt heating of matrix crystals. In the matrix crystals, the dielectric effect reduced reaction Gibbs free energy under typical MALDI conditions. The result suggested that thermal energy plays an important role in the initial ionization reaction of THAP.

Matrix-assisted laser desorption/ionization (MALDI) is an important volatilization and ionization technique for large biomolecules,[1,2] but the ionization mechanism is not clearly understood. Because of a lack of complete information on the ionization process, the method is rife with problems such as the choice of proper matrices and sample preparation protocols. It is also difficult to conduct quantitative analyses because of heterogeneous sample morphologies. Although numerous theoretical models and experimental investigations have been conducted to explain the mechanism,[3–9] a unified reaction model has not been found. In order to overcome the limitations which exist when using MALDI, it is important to analyze critical initial reactions in further detail.

Throughout the reaction details proposed in the literature, a major question is how initial ions are generated. Prevailing theoretical models can be briefly categorized into two distinct categories: (a) the non-linear photoionization model, and (b) the Lucky Survivor (LS) model. The non-linear photoionization model was initiated by Ehring *et al.* by emphasizing the essential role of a highly electronically excited matrix.[6] Since the two-photon energy of the commonly used laser in MALDI was usually insufficient to ionize free matrix molecules,[10] a two-step process was proposed to overcome ionization energy. By laser irradiation, matrix radical cations (which in turn underwent chemical reactions with neutral molecules to produce a protonated matrix) were proposed to be formed in annihilation processes.[6,11] Although the annihilation model adequately explains the ionization of fluorescent matrixes with a first excited-state lifetime (τ_1) of nanoseconds,[11,12] it is difficult to explain the ionization of matrixes with τ_1 in the low picosecond range or shorter,[13,14] such as sinapinic acid (SA) and 2,4,6-trihydroxyacetophenone (THAP). In contrast to the non-linear photoionization model, Karas *et al.* emphasized the contribution of pre-charged ions in the LS model.[4] In this model, analytes incorporated into the matrix crystal preserved their charge states acquired in sample solution, and became singly charged free molecules by neutralizing with counter ions during the desorption

* *Correspondence to:* Y.-S. Wang, Genomics Research Center, Academia Sinica, Taipei 115, Taiwan.
E-mail: wer@gate.sinica.edu.tw
** *Correspondence to:* S. H. Lin, Institute of Atomic and Molecular Sciences, Academia Sinica, Taipei 10617, Taiwan.
E-mail: sheng@mail.nctu.edu.tw

Rapid Communications in Mass Spectrometry

process.[4] The LS model essentially accounts for many phenomena observed in MALDI, but it is difficult to apply to matrices that are neutral in solution, such as THAP. Moreover, the source of photoelectrons that play an essential role in charge neutralization was not clearly described in the LS model.[15] In fact, it is difficult to establish a universal model accounting for all the conditions of MALDI because the result depends on the chemical properties of individual matrices, the sample preparation method, and excitation conditions.[16,17]

Among commonly used matrices, THAP represents a unique matrix as it cannot be well explained by most existing models. An interesting observation of THAP was that its laser-induced infrared emission was higher than many popular matrixes even though its absorption cross section at the excitation wavelength was low.[16] Because the non-radiative relaxation channel dominates in THAP, significant photon energy is converted into thermal energy when returning back to its ground state. Since proton disproportionation is predicted to be energetically more favorable than photoionization,[3] THAP becomes an ideal molecule for the study of proton disproportionation energetics under the high-temperature MALDI conditions. A recent study also concluded that proton disproportionation is a thermal process.[9] Although an intramolecular proton transfer mechanism from ortho-OH to the carboxyl group was thought to be responsible for proton disproportionation,[18] a more general explanation is still necessary for molecules without ortho-OH groups, such as THAP or SA.

In this paper, an extended work was conducted to study the contribution of thermal energy to the initial reaction in MALDI. A quantitative model was proposed to describe proton disproportionation of solid THAP. Experiments were conducted to analyze ionic and desorbed neutral molecules of THAP at the near threshold fluence of a 355 nm laser. The chemical equilibrium between ions and neutral molecules as well as the desorption process were proposed on the basis of the observations from the current work and another study.[19] Since the initial reaction was presumed to occur in the condensed phase, quantum chemistry calculations with dielectric effect were conducted to evaluate the reaction Gibbs free energy (ΔG) of proton disproportionation. A similar concept has been discussed previously.[9,18] To further probe the contribution of thermal energy with minimum side reactions, a mixture of THAP and fullerene (C_{60}) was irradiated by a 450 nm laser to selectively excite chemically inert C_{60}. Such carbon materials have been used as matrices for ionizing low molecular weight species,[20–22] and C_{60} produces the least interference in the low molecular range. Under 450 nm laser, proton disproportionation of THAP can only be induced by thermal energy from C_{60} because the electronic transitions of THAP at this wavelength are inactive.

EXPERIMENTAL

All chemicals were of analytical grade and purchased from Sigma-Aldrich Chemical Corporation. THAP was dissolved in 50% aqueous acetonitrile solution to a concentration of 0.1 M. The matrix solution was then dropped on the sample target and vacuum-dried to a final amount of 200 nmol. For the experiment involving a mixture of C_{60} and THAP, C_{60} was first dissolved in toluene to a concentration of 5×10^{-3} M and deposited on the sample target. After rapid vacuum-drying, the THAP solution was dropped and vacuum-dried on the C_{60} layer to a C_{60}-to-THAP molar ratio of 2000. The high C_{60}-to-THAP molar ratio assured THAP was in intimate contact with C_{60}.

The dependence of desorbed neutral molecule abundance on laser fluence was measured by a crossed-molecular beam machine. The specific features of the machine developed for this experiment are shown in Fig. 1 while the remaining details are given elsewhere.[23] Pressures in the main and detector chambers were approximately 10^{-6} and 10^{-10} Torr, respectively. A pair of openings (8 mm in diameter) was installed at the entrance of the detector chamber to limit the conductance of residual gas. The MALDI samples were transferred to the surface of a rotatable stainless steel sample holder positioned at the center of the main chamber. A frequency-tripled Nd:YAG laser beam (355 nm, pulse width ~5 ns, MINILITE I, Continuum) was used to irradiate the sample surface at about 45° from the surface normal. The laser beam was focused by a fused silica lens (f = 30 cm) installed inside the vacuum chamber, resulting in a circular spot roughly 250 μm in diameter. Laser energy was regulated by a circular neutral-density filter and monitored by a pyroelectric energy meter (PEM 100, LTB Lasertechnik). Experiments were performed under a laser fluence of 75 to 340 J m^{-2}. The detector chamber was located 350 mm away from the sample surface. It comprised an electron impact ionizer of 70 eV ionization energy, a quadrupole mass filter, and a Daly-type ion counter. The detector chamber was rotatable about the sample surface, and the desorbed neutral species were measured at 0, 15, 30, 45, 60, and 75° from the normal of the sample surface. Angular correction was

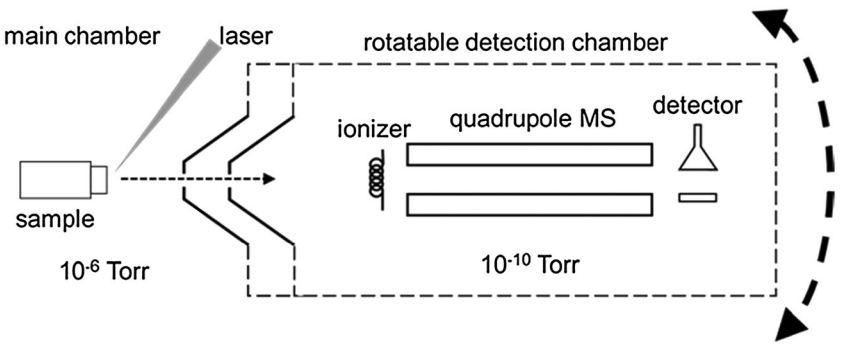

Figure 1. Schematics of the mass spectrometer for detection of desorbed neutral products.

conducted to calculate neutral abundance and the time-of-flight profile of ions was used to analyze the correlation between different ions. Every data point was averaged over 15 to 1000 shots from fresh sample areas, depending on laser fluence. To eliminate electronic and chemical noise, blank calibration was conducted by following the above same data acquisition procedure without turning on the electron impact ionizer.

The dependence of MALDI ion abundance on laser fluence was analyzed by a commercial MALDI-TOF mass spectrometer (Autoflex III, Bruker Daltonik) equipped with two external laser systems. For the pure THAP experiment, a frequency-tripled Nd:YAG laser (LS-2134, Lotis TII, 355 nm, pulse duration (FWHM) of 10–12 ns) was used. For the THAP and C_{60} mixture, 450 nm laser photons were generated with an Nd:YAG pumped Ti:Sapphire tunable laser (LT-2211, Lotis TII, pulse duration (FWHM) of 8–30 ns). The laser beams were both about 260 μm in diameter at the sample surface. Ions were detected without delayed extraction in reflectron mode. Every data point for both polarities was averaged from four mass spectra, where every spectrum was the sum of 200 individual laser shots. The initial accelerating voltage was 20 kV. Other instrument settings were fixed throughout measurements after optimization.

Standard Gibbs free energy (ΔG^0) and standard reaction entropy (ΔS^0) of the proton disproportionation of THAP were calculated with *GAUSSIAN 03* software. The entropy and temperature effects were included in the evaluation of the ΔG in the gas phase, whereas an additional dielectric effect was also used for evaluation in the condensed phase. Density functional theory (DFT) at the B3LYP level of theory was used to calculate the thermodynamic properties of the matrix. To achieve these computations, the 6-31 + g (d, p) basis set was used. To evaluate dielectric effect on the MALDI reaction, a polarizable continuum model (with a definition of a cavity by the united atom model for Hartree-Fock (PCM-UAHF)) was employed.[24] In the PCM-UAHF method, a molecule was placed into a defined cavity with a continuous dielectric medium to mimic a matrix crystallization environment. PCM-UAHF predicted reliably the hydration effect and the solvated free energy of neutral and charged species.[25]

RESULTS AND DISCUSSION

The quantitative thermal model

For a non-fluorescent matrix like THAP, the photon energy is mainly converted into thermal energy via ultrafast non-radiative relaxation. The conversion of the incident laser energy into lattice phonons[26,27] results in the abrupt overheating of the matrix crystal. The linear dependence of temperature on laser fluence can be derived from the heat equation:

$$T = T_0 + \gamma F \tag{1}$$

where T_0 and F represent the initial surface temperature and laser fluence, respectively, and γ is the conversion coefficient of laser fluence to temperature. The derivation of Eqn. (1) is described in the Supporting Information. This is consistent with the previous works of Dreisewerd *et al.*[7] and Koubenakis *et al.*[28]

High-temperature conditions induced phase transition and a high-pressure environment at tens to hundreds MPa.[26,29,30] The implications of this are that virtual thermodynamic and chemical equilibriums can be established efficiently by frequent collisions.[7,31] This is in contrast to the pseudoequilibrium presumption within a highly dynamic plume given in the literature.[5] A theoretical model has been developed previously,[19] in which the abundances of ionic matrix and analyte (I_P) depended on the concentration of corresponding species on the surface ($[P]_{(s)}$) and the desorption rate constant (k_{desorb}):

$$I_p \propto k_{desorb}[P]_{(S)} \tag{2}$$

On the basis of observations, a thermally induced proton disproportionation in the solid phase was postulated:

$$2THAP_{(S)} \overset{K_1}{\leftrightarrow} [THAP + H]^+_{(S)} + [THAP - H]^-_{(S)} \tag{3}$$

Proton disproportionation could be enhanced in the hydrogen bonding network of matrix crystals. Applying the desorption rate constant derived from transition state theory, the yield of desorbed neutral THAP and protonated/deprotonated THAP can be formulated by Eqns. (4) and (5), respectively,

$$I_{neutral} \propto \frac{k(T_0 + \gamma F)}{h} \times \left(1 - e^{\frac{-h\nu}{k(T_0+\gamma F)}}\right) \times e^{-\frac{\Delta E_a}{k(T_0+\gamma F)}} \times \frac{1}{1 + 2\sqrt{K_1}} \tag{4}$$

$$I_{ion} \propto \frac{k(T_0 + \gamma F)}{h} \times \left(1 - e^{\frac{-h\nu}{k(T_0+\gamma F)}}\right) \times e^{-\frac{\Delta E_a}{k(T_0+\gamma F)}} \times \frac{\sqrt{K_1}}{1 + 2\sqrt{K_1}} \tag{5}$$

in which $\sqrt{K_1}$ is a measure of the ion-to-neutral ratio in this model. It is a term used to determine the degree of ionization efficiency and relates to the ionization mechanism. Sublimation enthalpy (ΔE_a) of neutral THAP was adopted in Eqn. (5) since ions coexpanded with the vast majority of neutral molecules. However, the ion-to-neutral ratio should be discussed with caution because its value spans as many as six orders of magnitude (from 10^{-3} to 10^{-9}) in the literature,[9,32–35] due to differences in matrces, analytes, analyte-to-matrix ratio, preparation method, laser energy, wavelength, laser beam profile, and detection method.[36–39] Furthermore, interactions between matrices and analytes like hydrogen bonding networks also affect the ionization efficiency of analytes.[40]

Desorbed neutral THAP with 355 nm pulse laser

Desorbed neutral species from pure THAP gave rise to major peaks of molecular cations at *m/z* 168, the abundant fragment at *m/z* 153, and minor peaks at *m/z* 69, 43, and others.[41] These fragment ions were attributed to decomposed products resulting from electron impact ionization as they all had the same time-of-flight profile.[42] The two major peaks (*m/z* 168 and 153) were summed for subsequent modeling and plotted as a function of laser fluence in Fig. 2. Even though the ion-to-neutral ratio cannot be determined precisely, most of the values reported in the literature were small enough to approximate the concentration portion of Eqn. (4) to unity to obtain Eqn. (6).

$$I_{neutral} \propto \frac{k(T_0 + \gamma F)}{h} \times \left(1 - e^{\frac{-h\nu}{k(T_0+\gamma F)}}\right) \times e^{-\frac{\Delta E_a}{k(T_0+\gamma F)}} \tag{6}$$

The sublimation enthalpy (ΔE_a) of THAP was predicted to be 100 kJ mol^{-1} by the quantitative structure property relationship (QSPR) model,[43] and fitting parameters, γ of

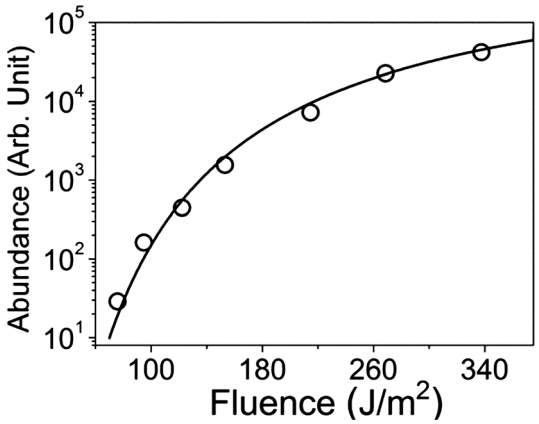

Figure 2. Desorbed neutral THAP as a function of 355 nm laser fluence. Open circles are experimental data (counting per laser shot). Solid line is the fitting result from Eqn. (6) with ΔE_a of 100 kJ mol^{-1} and γ of 10.9 $K\,m^2\,J^{-1}$.

10.9 ($K\,m^2\,J^{-1}$) and v of 350 cm^{-1}, were used, as discussed in previous works.[16,19] Notably, v is the vibrational frequency of the intermolecular bond from the vibrational partition function of transition state theory, and 350 cm^{-1} is a typical value for non-covalent interactions in organic solids. It needs to be emphasized that sublimation energy makes a significant contribution to the fitted result and should not be adjusted arbitrarily. For compounds of no experimental data, the QSPR model provides reliable values. Based on these fitting parameters, the resulting theoretical prediction agreed well with observations (Fig. 2).

Herein, with the γ value determined from neutral desorption and initial temperature-dependent experiments, a maximum temperature of about 1900 K was estimated for a laser fluence of 150 $J\,m^{-2}$, or 1388 K for 100 $J\,m^{-2}$ (a typical MALDI laser fluence for other matrices). Notably, the higher temperature is exclusively for THAP while the lower temperature can be derived from other matrices. The difference relates to the distinct chemical and thermodynamic properties. Furthermore, in these experiments, abrupt overheating was retarded by expansion cooling and other endothermic reactions.[16,44] Notably, there is little consensus on MALDI temperatures[7,28,44–48] due to a lack of reliable temperature detection techniques. This means that in order to conduct more reliable quantitative analyses in the future, improvements in temperature measurement are necessary.

Thermally induced initial reaction of THAP

Proton disproportionation of THAP was presumed to be the major initial reaction because protonated/deprotonated THAP dominates under typical MALDI conditions. The results of the laser fluence dependence experiments revealed that protonated and deprotonated THAP have nearly the same threshold fluence and pair-wise intensity. This agreed with the reaction predicted in Eqn. (3). The absence of radical ions also supported the assumption that the non-linear photoionization is inefficient for THAP excited by a 355 nm laser.[16] Since proton disproportionation in the excited state is uncommon among popular matrices,[49] it is most likely to occur in the ground state. Notably, quantum chemistry calculations of energetics of Eqn. (3) for the basis set used in this work yielded only a 0.4% error with respect to the experimental value (4.89 eV for gaseous THAP).[50]

Electrostatic interactions or dielectric effects exist because most commonly used matrices have unbalanced charge distributions. These interactions are critical to the structure and energy of a molecule in the condensed phase (molecules are tightly surrounded by the same molecules) as they assisted in stabilizing ion species. Such effects should be considered in the evaluation of ΔG in the condensed phase.[9,18] Since the dielectric constant of THAP is unknown, ΔG of Eqn. (3) was evaluated from the calculation of a series of dielectric values. The ΔG^0 and the ΔS^0 values of the corresponding dielectric constants are listed in Supplementary Table S1 (Supporting Information). As shown in Fig. 3 and Table S1, a ΔG^0 of 4.91 eV was obtained for THAP in the gas phase and the reaction enthalpy decreased as the dielectric constant increased. The calculated ΔG^0 dropped to 3.54 eV when a dielectric constant of 2.38 was used in calculations, which can be overcome by the energy of a single photon from conventional MALDI lasers. Approximately half of the ΔG^0 of the gas-phase value (52.5%) was obtained at a dielectric constant of 5.62. The decline in the ΔG^0 leveled off when a dielectric constant of above ten was used, suggesting that the ΔG^0 reached an equilibrium value. Among molecules with a dielectric constant available, acetophenone has the nearest structure to THAP and its dielectric constant is 17.44,[51] but the value of THAP is likely higher because it is more polar than acetophenone.

Dielectric effect is important under typical MALDI temperature, even when the dielectric constant decreases as temperature increases. Extrapolating the dielectric constant from room temperature to a typical MALDI temperature results in a reduction of the value by about 50%.[5] To account for additional parameters affecting this value, such as pressure, a final value of roughly 5.62 was used, a value that is two-thirds the original value. Applying this value of the dielectric constant in Eqn. (5), the resultant ΔG^0 is 2.58 eV and ΔS^0 is 28.11 $J\,mol^{-1}\,K^{-1}$ (see Supporting Information for additional details). As shown in Fig. 4, the prediction from the quantitative thermal model agreed with the observed protonated/deprotonated THAP signals except for a fluence regime higher than 350 $J\,m^{-2}$. The presumed reasons for the discrepancy in the high fluence regime was the loss of ion signals due to the severe divergence of the ion beam,[19] and the abundance of THAP dimers and fragments that were disregarded in the analysis.

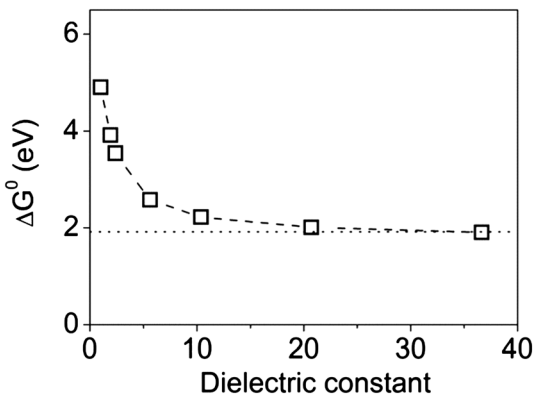

Figure 3. Dependence of the standard Gibbs free energy (ΔG^0) of the proton disproportionation reaction on dielectric constant.

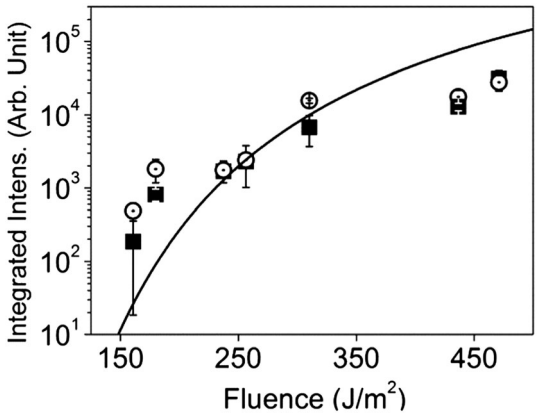

Figure 4. Desorbed ionic product intensity as a function of 355 nm laser fluence. The solid squares represent $[THAP + H]^+$, the open circles stand for $[THAP–H]^-$, and the solid line is the theoretical prediction calculated with Eqn. (5).

With regard to energy requirements, thermal ionization is apparently a significant pathway for THAP, and may also play a role in other matrices. The same conclusion was also made by Beavis and Chait and co-workers on the basis of strikingly similar results between UV- and IR-MALDI mass spectra;[27,52] however, more work is needed to verify thermal contribution to IR MALDI since other mechanisms may influence this contribution.[53]

Desorbed ions from mixture of THAP and C_{60} at 450 nm

The thermal ionization of THAP was further verified by mixing THAP with pristine C_{60} to produce a high-temperature condition while minimizing the electronic transition of THAP. Notably, the protonated/deprotonated THAP can be obtained by 450 nm laser only when mixing with C_{60} as demonstrated in the current work. The excitation wavelength was 450 nm since C_{60} exhibits a broad absorption band to the visible range whereas the absorption of THAP is almost zero.[16,54] Under such conditions, THAP cannot be a successful matrix since high optical absorption at the excitation laser wavelength is a prerequisite of MALDI.[4,6,39] This was confirmed by a measurement showing no ion was produced from pure THAP, in this experiment the THAP was prepared on a stainless steel surface covered by a dielectric film (double-sided tape) to minimize any interference from the metal substrate. After pumping by 450 nm photons, C_{60} undergoes electronic excitation. This was followed by internal conversion and intersystem crossing to triplet states.[55] With ultrafast intramolecular relaxation, triplet-triplet annihilation,[56–58] and negligible fluorescence relaxation at ambient temperature,[59] C_{60} served as a "thermal energy generator" activating thermal THAP reactions. Figures 5(a) and 5(b) show protonated/deprotonated THAP dominant peaks and they are separated from those of C_{60} cation and anion radicals. The spectra are very similar to those obtained for pure THAP at 355 nm displayed in the insets. Moreover, protonated/deprotonated THAP also appear to be pair-wise, as shown in Fig. 5(c), which is also similar to the results of pure THAP excited by 355 nm laser. These results provide indirect support and are consistent with a previous study showing a significant thermal contribution to proton disproportionation in THAP.[16]

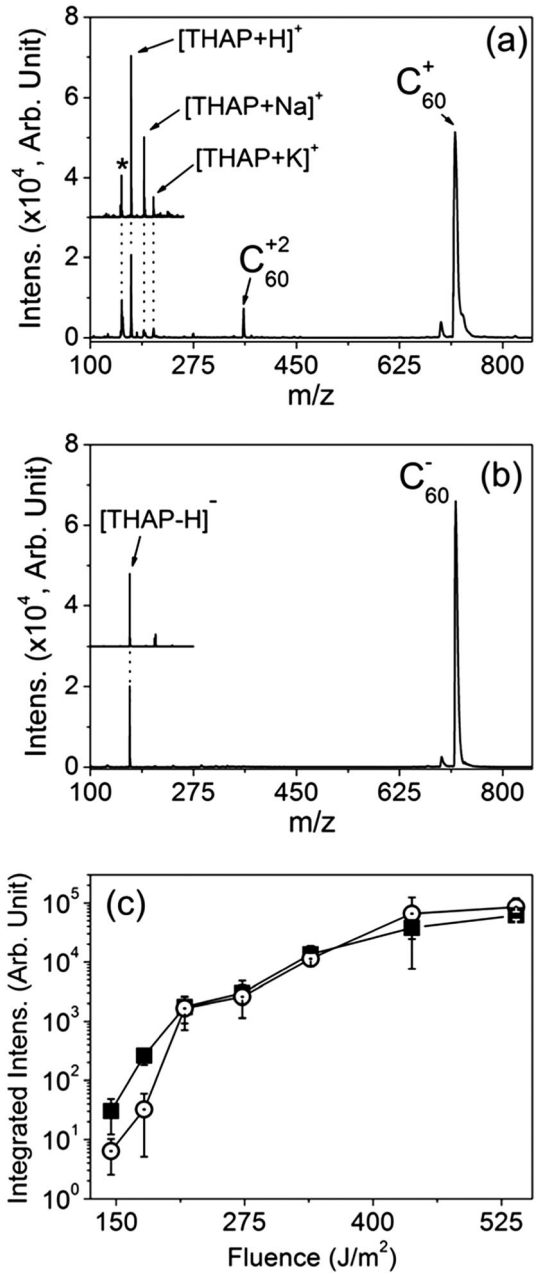

Figure 5. Mass spectra obtained from the mixture of THAP and C_{60} in (a) positive ion mode and (b) negative ion mode. Laser fluence was 340 J m^{-2}. Insets in (a) and (b) are the typical mass spectra of pure THAP at 355 nm in positive and negative mode, respectively. The asterisk indicates the fragment of THAP. (c) Dependence of protonated (solid squares) and deprotonated (open circles) THAP on laser fluence.

It is worth noting that although possible interaction channels between C_{60} ions and THAP cannot be completely ruled out, such as interactions between the photoelectrons emitted from C_{60} with THAP to yield THAP radical ions, the contribution of such reactions was not detected in the current study. This is presumably due to the significantly higher electron affinity of C_{60} (2.65 eV)[60] than that of common matrices (1 eV or less).[5] The dominant ionic radical pair of C_{60} is attributed to an energetically favorable electron disproportionation reaction[58] and the high C_{60}-to-THAP

molar ratio. No evidence of electron transfer reactions between THAP and C_{60} ionic radicals was observed under the current experimental conditions. There was no radical ions of THAP produced in the current study, suggesting that the ionization condition was similar to that the pure THAP excited by 355 nm laser. These results reveal the important role of thermal energy to the initial reaction of THAP.

CONCLUSIONS

A quantitative thermal ionization model was established to explain the initial reaction of THAP. The irradiated matrix region reached thermodynamic equilibrium due to ultrafast non-radiative relaxation and a large number of collisions. An Arrhenius-type desorption rate constant derived from transition state theory was used to formulate the desorption process. This mathematical formula encompassing ionization and desorption describes not only THAP ions, but also neutral THAP molecules as a function of laser fluence. Dielectric effect was considered in evaluating the ΔG since the initial reaction occurs in the condensed phase. The calculation indicated that the reaction enthalpy of proton disproportionation of THAP with dielectric effect could be overcome by thermal energy generated from a single UV laser photon. The mass spectrum of THAP obtained from the mixture of THAP and C_{60} at 450 nm was in support of a thermally induced initial reaction. Quite apart from other ionization pathways, the results herein reveal the important contribution of thermal-induced chemical reactions in MALDI. It needs to be emphasized, however, that other mechanisms should not be ruled out owing to the specific photochemical properties of matrices as well as excitation conditions. Further development of the thermal ionization model to help interpret the ionization of alkali metal impurities is important because these impurities produce alkali-ion adducts of analytes and other chemical noise. A quantitative analysis of alkali-ion adducts of carbohydrates will be discussed in subsequent works.

Acknowledgements

This work was supported by the Genomics Research Center and the Institute of Atomic and Molecular Sciences, Academia Sinica. Financial support from the National Science Council of Taiwan (Contract No. 101-2113-M-001-003-MY3) is also acknowledged.

REFERENCES

[1] M. Karas, F. Hillenkamp. Laser desorption ionization of proteins with molecular masses exceeding 10 000 daltons. *Anal. Chem.* **1988**, *60*, 2299.
[2] K. Tanaka, H. Waki, Y. Ido, S. Akita, Y. Yoshida, T. Yoshida. Protein and polymer analyses up to *m/z* 100 000 by laser ionization time-of-flight mass spectrometry. *Rapid Commun. Mass Spectrom.* **1988**, *2*, 151.
[3] R. Zenobi, R. Knochenmuss. Ion formation in MALDI mass spectrometry. *Mass Spectrom. Rev.* **1998**, *17*, 337.
[4] M. Karas, R. Kruger. Ion formation in MALDI: The cluster ionization mechanism. *Chem. Rev.* **2003**, *103*, 427.
[5] R. Knochenmuss. Ion formation mechanisms in UV-MALDI. *Analyst* **2006**, *131*, 966.
[6] H. Ehring, M. Karas, F. Hillenkamp. Role of photoionization and photochemistry in ionization processes of organic molecules and relevance for matrix-assisted laser desorption ionization mass spectrometry. *Org. Mass Spectrom.* **1992**, *27*, 472.
[7] K. Dreisewerd, M. Schurenberg, M. Karas, F. Hillenkamp. Influence of the laser intensity and spot size on the desorption of molecules and ions in matrix-assisted laser desorption/ionization with a uniform beam profile. *Int. J. Mass Spectrom.* **1995**, *141*, 127.
[8] D. A. Allwood, P. E. Dyer, R. W. Dreyfus. Ionization modelling of matrix molecules in ultraviolet matrix-assisted laser desorption/ionization. *Rapid Commun. Mass Spectrom.* **1997**, *11*, 499.
[9] Y. J. Bae, Y. S. Shin, J. H. Moon, M. S. Kim. Degree of ionization in MALDI of peptides: Thermal explanation for the gas-phase ion formation. *J. Am. Soc. Mass Spectrom.* **2012**, *23*, 1326.
[10] S. Bourcier, Y. Hoppilliard. B3LYP DFT molecular orbital approach, an efficient method to evaluate the thermochemical properties of MALDI matrices. *Int. J. Mass Spectrom.* **2002**, *217*, 231.
[11] R. Knochenmuss. A quantitative model of ultraviolet matrix-assisted laser desorption/ionization. *J. Mass Spectrom.* **2002**, *37*, 867.
[12] H. C. Ludemann, R. W. Redmond, F. Hillenkamp. Singlet-singlet annihilation in ultraviolet matrix-assisted laser desorption/ionization studied by fluorescence spectroscopy. *Rapid Commun. Mass Spectrom.* **2002**, *16*, 1287.
[13] T. Hoyer, W. Tuszynski, C. Lienau. Ultrafast photodimerization dynamics in α-cyano-4-hydroxycinnamic and sinapinic acid crystals. *Chem. Phys. Lett.* **2007**, *443*, 107.
[14] R. Yamamoto, T. Fujino. 2,4,6-Trihydroxyacetophenone on zeolite surface: Correlation between electronic relaxation and fragmentation on mass spectra. *Chem. Phys. Lett.* **2012**, *543*, 76.
[15] B. H. Liu, O. P. Charkin, N. Klemenko, C. W. Chen, Y. S. Wang. Initial ionization reaction in matrix-assisted laser desorption/ionization. *J. Phys. Chem. B* **2010**, *114*, 10853.
[16] Y.-H. Lai, C.-C. Wang, C. W. Chen, B.-H. Liu, S. H. Lin, Y. T. Lee, Y.-S. Wang. Analysis of initial reactions of maldi based on chemical properties of matrixes and excitation condition. *J. Phys. Chem. B* **2012**, *116*, 9635.
[17] T. W. Jaskolla, M. Karas. Compelling evidence for lucky survivor and gas phase protonation: The unified maldi analyte protonation mechanism. *J. Am. Soc. Mass Spectrom.* **2011**, *22*, 976.
[18] K. Murakami, A. Sato, K. Hashimoto, T. Fujino. Study of ionization process of matrix molecules in matrix-assisted laser desorption ionization. *Chem. Phys.* **2013**, *419*, 37.
[19] Y.-H. Lai, C.-C. Wang, S.-H. Lin, Y.-T. Lee, Y.-S. Wang. Solid-phase thermodynamic interpretation of ion desorption in matrix-assisted laser desorption/ionization. *J. Phys. Chem. B* **2010**, *114*, 13847.
[20] L. Michalak, K. J. Fisher, D. S. Alderdice, D. R. Jardine, G. D. Willett. C_{60}-assisted laser desorption-ionization mass spectrometry. *Org. Mass Spectrom.* **1994**, *29*, 512.
[21] C. Black, C. Poile, J. Langley, J. Herniman. The use of pencil lead as a matrix and calibrant for matrix-assisted laser desorption/ionisation. *Rapid Commun. Mass Spectrom.* **2006**, *20*, 1053.
[22] Z. Szabo, R. M. Vallant, A. Takatsy, R. Bakry, M. Najam-ul-Haq, M. Rainer, C. W. Huck, G. K. Bonn. Laser desorption/ionization mass spectrometric analysis of small molecules using fullerene-derivatized silica as energy-absorbing material. *J. Mass Spectrom.* **2010**, *45*, 545.
[23] Y. T. Lee, J. D. McDonald, P. R. Lebreton, D. R. Herschba. Molecular beam reactive scattering apparatus with electron bombardment detector. *Rev. Sci. Instrum.* **1969**, *40*, 1402.

[24] J. Tomasi, B. Mennucci, R. Cammi. Quantum mechanical continuum solvation models. *Chem. Rev.* **2005**, *105*, 2999.
[25] V. Barone, M. Cossi, J. Tomasi. A new definition of cavities for the computation of solvation free energies by the polarizable continuum model. *J. Chem. Phys.* **1997**, *107*, 3210.
[26] L. V. Zhigilei, E. Leveugle, B. J. Garrison, Y. G. Yingling, M. I. Zeifman. Computer simulations of laser ablation of molecular substrates. *Chem. Rev.* **2003**, *103*, 321.
[27] X. J. Chen, J. A. Carroll, R. C. Beavis. Near-ultraviolet-induced matrix-assisted laser desorption/ionization as a function of wavelength. *J. Am. Soc. Mass Spectrom.* **1998**, *9*, 885.
[28] A. Koubenakis, V. Frankevich, J. Zhang, R. Zenobi. Time-resolved surface temperature measurement of maldi matrices under pulsed uv laser irradiation. *J. Phys. Chem. A* **2004**, *108*, 2405.
[29] R. Knochenmuss, L. V. Zhigilei. Molecular dynamics simulations of MALDI: Laser fluence and pulse width dependence of plume characteristics and consequences for matrix and analyte ionization. *J. Mass Spectrom.* **2010**, *45*, 333.
[30] R. Srinivasan, B. Braren. Ultraviolet laser ablation of organic polymers. *Chem. Rev.* **1989**, *89*, 1303.
[31] Y. Minegishi, D. Morimoto, J. Matsumoto, H. Shiromaru, K. Hashimoto, T. Fujino. Desorption dynamics of tetracene ion from tetracene-doped anthracene crystals studied by femtosecond time-resolved mass spectrometry. *J. Phys. Chem. C* **2012**, *116*, 3059.
[32] A. P. Quist, T. Huthfehre, B. U. R. Sundqvist. Total yield measurements in matrix-assisted laser desorption using a quartz crystal microbalance. *Rapid Commun. Mass Spectrom.* **1994**, *8*, 149.
[33] C. D. Mowry, M. V. Johnston. Simultaneous detection of ions and neutrals produced by matrix-assisted laser desorption. *Rapid Commun. Mass Spectrom.* **1993**, *7*, 569.
[34] W. Ens, Y. Mao, F. Mayer, K. G. Standing. Properties of matrix-assisted laser desorption measurements with a time-to-digital converter. *Rapid Commun. Mass Spectrom.* **1991**, *5*, 117.
[35] M.-T. Tsai, S. Lee, I. C. Lu, K. Y. Chu, C.-W. Liang, C. H. Lee, Y. T. Lee, C.-K. Ni. Ion-to-neutral ratio of 2,5-dihydroxybenzoic acid in matrix-assisted laser desorption/ionization. *Rapid Commun. Mass Spectrom.* **2013**, *27*, 955.
[36] R. C. Beavis, B. T. Chait. High-accuracy molecular mass determination of proteins using matrix-assisted laser desorption mass spectrometry. *Anal. Chem.* **1990**, *62*, 1836.
[37] O. Vorm, P. Roepstorff, M. Mann. Improved resolution and very high sensitivity in maldi tof of matrix surfaces made by fast evaporation. *Anal. Chem.* **1994**, *66*, 3281.
[38] H. Qiao, V. Spicer, W. Ens. The effect of laser profile, fluence, and spot size on sensitivity in orthogonal-injection matrix-assisted laser desorption/ionization time-of-flight mass spectrometry. *Rapid Commun. Mass Spectrom.* **2008**, *22*, 2779.
[39] K. Dreisewerd. The desorption process in MALDI. *Chem. Rev.* **2003**, *103*, 395.
[40] V. Horneffer, M. Gluckmann, B. Kruger, M. Karas, K. Strupat, F. Hillenkamp. Matrix-analyte-interaction in MALDI-MS: Pellet and nano-electrospray preparations. *Int. J. Mass Spectrom.* **2006**, *249*, 426.
[41] NIST Chemistry WebBook. http://webbook.nist.gov/chemistry/.
[42] C.-W. Liang, C.-H. Lee, Y.-T. Lee, C.-K. Ni. Plume expansion dynamics of matrix-assisted laser desorption ionization. *Chem.-Asian J.* **2011**, *6*, 2986.
[43] F. Gharagheizi. A new molecular-based model for prediction of enthalpy of sublimation of pure components. *Thermochim. Acta* **2008**, *469*, 8.
[44] Y. J. Bae, J. H. Moon, M. S. Kim. Expansion cooling in the matrix plume is under-recognized in maldi mass spectrometry. *J. Am. Soc. Mass Spectrom.* **2011**, *22*, 1070.
[45] R. Knochenmuss, L. V. Zhigilei. What determines MALDI ion yields? A molecular dynamics study of ion loss mechanisms. *Anal. Bioanal. Chem.* **2012**, *402*, 2511.
[46] G. H. Luo, I. Marginean, A. Vertes. Internal energy of ions generated by matrix-assisted laser desorption/ionization. *Anal. Chem.* **2002**, *74*, 6185.
[47] E. Schulz, M. Karas, F. Rosu, V. Gabelica. Influence of the matrix on analyte fragmentation in atmospheric pressure MALDI. *J. Am. Soc. Mass Spectrom.* **2006**, *17*, 1005.
[48] C. D. Mowry, M. V. Johnston. Internal energy of neutral molecules ejected by matrix-assisted laser desorption. *J. Phys. Chem.* **1994**, *98*, 1904.
[49] V. Karbach, R. Knochenmuss. Do single matrix molecules generate primary ions in ultraviolet matrix-assisted laser desorption/ionization. *Rapid Commun. Mass Spectrom.* **1998**, *12*, 968.
[50] K. Breuker, R. Knochenmuss, R. Zenobi. Gas-phase basicities of deprotonated matrix-assisted laser desorption/ionization matrix molecules. *Int. J. Mass Spectrom.* **1999**, *184*, 25.
[51] *CRC Handbook of Chemistry and Physics: A Ready-Reference Book of Chemical and Physical Data*. CRC Press, Boca Raton, **2006**.
[52] S. F. Niu, W. Z. Zhang, B. T. Chait. Direct comparison of infrared and ultraviolet wavelength matrix-assisted laser desorption/ionization mass spectrometry of proteins. *J. Am. Soc. Mass Spectrom.* **1998**, *9*, 1.
[53] K. Dreisewerd, S. Berkenkamp, A. Leisner, A. Rohlfing, C. Menzel. Fundamentals of matrix-assisted laser desorption/ionization mass spectrometry with pulsed infrared lasers. *Int. J. Mass Spectrom.* **2003**, *226*, 189.
[54] K. Pichler, S. Graham, O. M. Gelsen, R. H. Friend, W. J. Romanow, J. P. McCauley, N. Coustel, J. E. Fischer, A. B. Smith. Photophysical properties of solid films of fullerene, C_{60}. *J. Phys.-Condes. Matter* **1991**, *3*, 9259.
[55] A. G. Stepanov, M. T. Portella-Oberli, A. Sassara, M. Chergui. Ultrafast intramolecular relaxation of C_{60}. *Chem. Phys. Lett.* **2002**, *358*, 516.
[56] N. M. Dimitrijevic, P. V. Kamat. Triplet excited state behavior of fullerenes: Pulse radiolysis and laser flash photolysis of C_{60} and C_{70} in benzene. *J. Phys. Chem.* **1992**, *96*, 4811.
[57] T. W. Ebbesen, K. Tanigaki, S. Kuroshima. Excited-state properties of C_{60}. *Chem. Phys. Lett.* **1991**, *181*, 501.
[58] C. C. Yang, K. C. Hwang. Disproportionation of photoexcited C_{60}. *J. Am. Chem. Soc.* **1996**, *118*, 4693.
[59] B. Ma, Y. P. Sun. Fluorescence spectra and quantum yields of [60]fullerene and [70]fullerene under different solvent conditions. A quantitative examination using a near-infrared-sensitive emission spectrometer. *J. Chem. Soc., Perkin Trans. 2* **1996**, 2157.
[60] V. Decoulon, J. L. Martins, F. Reuse. Electronic structure of neutral and charged C_{60} clusters. *Phys. Rev. B* **1992**, *45*, 13671.

SUPPORTING INFORMATION

Additional supporting information may be found in the online version of this article at the publisher's website.

